

ARTICLE

Supplementary Materials for

Supramolecular Net-Suppressor drives tumor vascular-immune microenvironment remodeling with spatiotemporal synchronization for Renal Cancer Therapy

Jiaqi Wang^{†,a,c}, Xiao Jin^{†,b}, Xiuhai Wu^{†,a,c}, Yu Wang^{†,e}, Xi Sun^{†,b}, Jiaye Li^a, Yue Teng^a, Yishuo Yan^a, Cong Li^a, Yulin Lv^c, Lingrui Jian^b, Kaiqiang Yuan^a, Lu Wang^{b,*}

^{a.} Department of Urology, Harbin Medical University Cancer Hospital, Harbin 150081, China

^{b.} The Fourth Affiliated Hospital of Harbin Medical University, Harbin 150001, China

^{c.} NHC Key Laboratory of Molecular Probes and Targeted Theranostics, Harbin Medical University, Harbin, 150001, China.

^{d.} Department of Urology, the 2nd Affiliated Hospital of Harbin Medical University, Harbin 150001, China

^{e.} Henan Institute of Advanced Technology, Zhengzhou University, No.100 Science Avenue, Zhengzhou 450052, China.

Experimental

Materials.

The mice renal carcinoma cell line (Renca) and human embryonic kidney 293T cells (293T) was purchased from Procell Life Science & Technology Co., Ltd., Wuhan, China. Human umbilical vein endothelial cells (Huvvec) and the clear cell renal cell carcinoma 786O cell line were donated by the Fourth Affiliated Hospital of Harbin Medical University. Roswell Park Memorial Institute 1640 medium (RPMI-1640), Dulbecco's Modified Eagle Medium (DMEM), fetal bovine serum (FBS), trypsin, penicillin/streptomycin, and phosphate buffered saline (PBS) were all purchased from Wanlei Biotechnology Co., Ltd., Nanjing, China. Peptides based RING were purchased from GL Biochem (Shanghai) Ltd., China. 96-well cell culture plates were purchased from Corning. Cell Counting Kit-8 (CCK-8) was purchased from Beyotime Institute of Biotechnology, Shanghai, China. 96-well enzyme-linked immunosorbent assay (ELISA) kits of IFN- γ , VCAM, ICAM were purchased from Solarbio Science & Technology Co., Ltd., Beijing, China. 3D spheroid culture plates (Ibidi GmbH, Germany). The cyanine dye was purchased from Yuanye Biotechnology Co., Ltd (Shanghai, China). Recombinant human VEGF and Tie2 protein were purchased from Sino Biological Inc. (Beijing, China). Axitinib was purchased from MedChemExpress (MCE, Shanghai, China), and the PD-L1 antibody used for treatment was obtained from Sino Biological Inc. (Beijing, China). All the other solvents used in the research were purchased from Solarbio Science & Technology Co., Ltd., Beijing, China and ZhaoKuiMuYan Co., Ltd., Beijing, China.

Molecular Synthesis.

Peptide molecules are synthesized using solid-phase peptide synthesis techniques based on Fmoc-coupling chemistry. The molecules were characterized by matrix-assisted laser desorption ionization time-of-flight mass spectrometry (MALDI-TOF-MS, Bruker Daltonics). In this study, an NHS ester-mediated amine labeling method was used to prepare cyanine dye peptides. The detailed procedures are described as follows: First, the polypeptides were dissolved in a Tris-HCl buffer at pH 8.5 to ensure the deprotonation of amino groups in the polypeptide molecules, thus providing optimal conditions for the subsequent reaction. Subsequently, Cy7-NHS esters were dissolved in anhydrous dimethyl sulfoxide (DMSO), and the resulting solution was slowly added dropwise to the aforementioned peptide solution under light-protected conditions at a ratio (mol/mol) of 10:3 (RING peptide to Cy7-NHS). The mixture was then stirred and reacted overnight at room temperature in the dark. After the reaction, the mixture was dialyzed against deionized water for 6 hours (cutoff: 1000 Da). Finally, the collected dialysate was freeze-dried. The dried fluorescent-labeled products were obtained, and then hermetically stored at -20 °C in the dark for subsequent use¹⁻³.

Surface Plasmon Resonance Imaging (SPR).

We used surface plasmon resonance imaging (SPR) technology to evaluate the interaction between the RING and VEGF or Tie2 protein. All SPR experiments were conducted using a Biacore S200 system. The SPR chip used was the Plexera® Nanocapture® chip, which has a bare gold layer with a thickness of 47.5 nanometers. Flow channel 1 on the sensor chip was designated as the reference channel, while channels 2, 3, and 4 served as the detection channels. VEGF/Tie2 was diluted to 1 mg/mL in 10 mM sodium acetate buffer (pH 4.0). The chip surface was first activated with 10 mmol/L solution of bis [succinimidyl propionate] disulfide (DSP) for 1 hour to attach amide groups. Protein immobilization was then performed for 10 minutes at a flow rate of 10 μ L/min. Subsequently, unreacted active sites on the chip surface were blocked with 5% bovine serum albumin (BSA). The same buffer was directed through the reference channel to maintain consistency. The immobilization buffer used was 1 \times HBS-EP (pH 7.4), containing 10 mM HEPES, 150 mM NaCl, 3 mM EDTA, and 0.005% (v/v) Tween-20. The SPR analysis process was carried out according to the following injection cycles: running buffer (PBS, used to stabilize the baseline); RING samples for binding assay (for VEGF interaction, RING peptide concentrations were: 12, 49, 98, 195, 391, 781, and 1563 nM, for Tie2 interaction, the peptide concentrations were: 6, 12, 24, 49, 98, 195, 391, and 781 nM); running buffer (PBS) for washing; 10 mmol/L glycine/hydrochloric acid buffer (pH = 2.5) for regeneration. The real-time binding signal was recorded and analyzed by the PlexArray HT system (Plexera LLC, Bothell, WA, USA). The dissociation constant (KD) was obtained by fitting the binding-dissociation curve using BIAevaluation software).

Transmission Electron Microscope (TEM) in Solution.

Morphology of RING molecules was characterized by TEM imaging. The solution of RING molecules (120 μ M, H₂O: DMSO = 99:1, v/v) w/wo the addition of vascular endothelial growth factor (VEGF) and tyrosine kinase with immunoglobulin-like and EGF-like domains 2 (Tie2) (at 0, 4, 8, 12 and 24 h) were dropcoated onto carbon-coated copper grids. Final concentration of VEGF and Tie2 was both 12 nM. After for 2 min, excess droplets were removed using filter papers. The TEM samples were dyed by uranyl acetate for another 1.5 min. All samples were dried under vacuum before the TEM observation.

Circular dichroism measurements.

Circular dichroism spectroscopy measurements were performed on a JASCO J-1500 spectropolarimeter with a 1 cm quartz cuvette at room temperature, with a spectral resolution of 0.1 nm for data acquisition. The solution baseline subtraction mode was selected in the instrument settings. For the experimental operation, a background solution of 1% hexafluoroisopropanol (HFIP) (H₂O: HFIP = 99:1, v/v) was first prepared to collect the baseline spectrum, followed by replacement with the sample solution for subsequent detection. At this point, the instrument directly outputted the spectrum of the sample with the baseline signal subtracted. The RING peptide was first dissolved in pure HFIP to

prepare a 12 mM stock solution, which was then diluted with deionized water to obtain a 120 μM working solution containing 1% HFIP (v/v) for subsequent experiments. For the induction assays, vascular endothelial growth factor (VEGF) and tyrosine kinase receptor 2 (Tie2) (both prepared at 12 nM in the same solvent described above) were mixed with the peptide solution at an equal volume ratio.

Fourier Transform Infrared (FTIR) Spectroscopy.

The polypeptide molecule RING1 was dissolved in water (120 μM , H_2O : DMSO = 99:1, v/v) with the incubation of VEGF and Tie2 (both 12 nM) for 12 h. The peptide-protein mixture was dropped onto a clean glass slide and air-dried to form a thin film for subsequent analysis. All samples were analyzed using the Spotlight 200i from PerkinElmer Instruments Co. Ltd.

Thioflavin T (ThT) assay.

The procedure for the Thioflavin T (ThT) assay was as follows: RING1 and RING2 peptides were each prepared as 120 μM solutions in PBS. All samples were sonicated at room temperature for 30 minutes and then filtered through a 0.22 μm membrane to remove pre-assemblies. RING peptide solution was transferred into black-walled 96-well plate (Corning 3603). Subsequently, these RING solution wells were aliquoted into two separate portions. For one part, 1 μL of PBS was added. To another one, 1 μL of a mixed protein solution containing VEGF and Tie2 (1.2 μM , PBS) was added as well. Then 1 μL of a ThT stock solution (2.5 mM, DMSO) was added into each well, and the mixture was allowed to stand for 30 minutes. Fluorescence measurements were initiated after above procedures. The fluorescence intensity was monitored using a microplate reader (SpectraMax iD3) with excitation at 450 nm and emission at 490 nm. A reading was taken every 2 minutes, and the monitoring continued for 2 hours. The measurement was stopped once the fluorescence signal reached a plateau. Finally, a scatter plot was generated using Origin software, with time plotted on the X-axis and fluorescence intensity on the Y-axis.

Critical aggregation concentration (CAC).

A pyrene stock solution with a concentration of approximately 2×10^{-4} M was prepared using acetone. A series of RING peptide solutions with sequentially increasing concentrations (20 μM , 40 μM , 60 μM , 80 μM , 100 μM , 200 μM , 300 μM , 400 μM) were prepared in H_2O : DMSO=99:1, v/v). 1 mL of the pyrene stock solution was added into a set of EP tubes. The acetone solvent was evaporated under a stream of air or nitrogen. Subsequently, 1 mL of the RING1 peptide solution at a specific concentration from the series was added to each tube. These samples were then divided into four experimental groups: RING1 alone, RING1 + VEGF, RING1 + Tie2, and RING1 + VEGF & Tie2. The final working concentrations of VEGF and Tie2 in the respective groups were 12 nM each. All sample vials were protected from light and incubated at a room temperature for 2 hours to allow for complete dissolution of pyrene and its partition into potential aggregates. Following incubation, fluorescence measurements were performed using a spectrofluorometer. The excitation spectrum of each sample was recorded over an emission wavelength range of 350–700 nm. Pyrene fluorescence emission shows a characteristic “five-finger” (five-peak) pattern. A plot was generated with the peptide concentration (on a logarithmic scale) on the x-axis and the fluorescence intensity ratio (I_{384}/I_{373}) on the y-axis. The CAC value for the RING1 peptide was determined from the intersection point of the trendlines using bilinear regression.

Cell Imaging using Confocal Laser Scanning Microscope.

The 786-O, 293T, and HUVEC cell lines were cultured in 1640 or DMEM medium containing 10% fetal bovine serum (FBS) and 1% antibiotic solution (penicillin and streptomycin) in an incubator at 37°C in a humidified atmosphere with 5% carbon dioxide. For HUVECs, binding assays were performed by being incubated with FITC-labeled RING1/2 (120 μM , medium: DMSO = 99:1 v/v) at 37°C for 45 minutes. After incubation, cells were washed with phosphate-buffered saline (PBS) and immediately imaged using confocal laser scanning microscopy (CLSM). For 786O cells, multicellular spheroids (MCSs) were generated to simulate three-dimensional tumor models. In retention assessment assay, these spheroids were incubated with FITC-labeled RING1/2 (120 μM) at 37°C for 8 hours. Following incubation, the drug solution was removed, MCSs were washed with PBS, and initial CLSM imaging was performed. The spheroids were then transferred to 96-well plates pre-coated with 2% agarose and cultured further. Imaging was repeated at designated time points to evaluate signal persistence. The 293T cell line, which expresses minimal VEGF and Tie2, served as a negative control. Both adherent and spheroid cultures were established followed by treatment and imaging procedures for binding assay. To assess self-assembly within spheroids, a Thioflavin T (ThT) fluorescence assay was conducted. Positive (786-O) and negative (293T) spheroids were incubated with RING1 or RING2 (120 μM) for 8 hours, washed with PBS to remove unbound peptide, and then incubated with ThT (25 μM) for 30 minutes at 37°C. After final PBS rinsing, spheroids were analyzed by CLSM to visualize ThT-positive β -sheet assemblies.

Mouse Subcutaneous Tumor Model and In Vivo Fluorescence Imaging.

All animal experiments were carried out in accordance with the “Guide for the Care and Use of Laboratory Animals”, which has been approved by the Animal Research Ethics Committee of the Fourth Affiliated Hospital of Harbin Medical University. To establish the Renca tumor-bearing mouse tumor model, 5×10^6 Renca cells in a cell suspension containing 50 μL of PBS mixed with 50 μL matrix gel were subcutaneously injected into the right back of female BALB/c mice (6 to 8 weeks old, weighing 18 to 22 grams). When the tumor volume on the right back of the mice was approximately 200 mm³, RING1 and RING2 (with a concentration of 400 μM , 200 μL prepared in PBS) were intravenously injected into the mice for the in vivo fluorescence imaging. After injection, the mice were scanned using a small animal in vivo imaging system (IVIS) at different time intervals (0.5, 4, 12, 24, 48, 60 and 72 h).

Frozen Tissue Sections and Fluorescent Imaging.

To verify the targeting ability of the polypeptide molecules in tumor tissue, Cy-labeled RING1/2 (400 μM) was injected into the tail vein of female BALB/c mice bearing Renca tumors (with a tumor size of approximately 200 mm^3). After 12 hours, tumor tissues were harvested, embedded in optimal cutting temperature (OCT) compound, and cryosectioned into 5 μm slices. For blocking, sections were incubated with 5% bovine serum albumin (BSA) for 30 minutes at room temperature. Primary antibodies against VEGF (1:100, Abcam, Cambridge, UK) and Tie2 (1:100, Abcam, Cambridge, UK) were applied overnight at 4 $^{\circ}\text{C}$ in a humidified chamber. After PBS washes, sections were incubated with Alexa Fluor 488-conjugated secondary antibodies for 1 hour at room temperature in the dark. Slides were washed and mounted with DAPI-containing antifade mounting medium. Imaging was performed using a CLMS.

To further evaluate biological markers within tumor tissues, separate tumor samples were fixed with 4% paraformaldehyde for 24 hours, embedded in paraffin, and sectioned into 5 μm slices. These sections were deparaffinized in xylene and rehydrated through graded ethanol series. For antigen retrieval, tissue sections were immersed in citrate buffer (pH 6.0) and heated using a microwave oven or pressure cooker. Tissue sections were then permeabilized with 0.3% Triton X-100 in PBS for 10 minutes, followed by blocking with 5% bovine serum albumin (BSA) for 30 minutes at room temperature to reduce nonspecific binding. Primary antibodies were applied overnight at 4 $^{\circ}\text{C}$ in a humidified chamber. The antibody panel included anti-CD31 (Wuhan Servicebio Technology Co., Ltd.), anti- α -SMA (Wuhan Servicebio Technology Co., Ltd.), and anti-NG2 (Cell Signaling Technology, Inc.) for tumor vasculature assessment; anti-CD8 (Wuhan Servicebio Technology Co., Ltd.), anti-interferon- γ (IFN- γ) (Wuhan Servicebio Technology Co., Ltd.), and anti-Granzyme B (Wuhan Servicebio Technology Co., Ltd.) for evaluating immune activation; as well as anti-22 (Abcam, Cambridge, UK), and anti-ZO-1 (Cell Signaling Technology, Inc.) to examine macrophage infiltration and vascular permeability. After PBS washes, sections were incubated with species-appropriate Alexa Fluor 488/647-conjugated secondary antibodies for 1 hour at room temperature in the dark. Nuclei were counterstained using DAPI-containing antifade mounting medium.

Cell Migration and Angiogenesis Assays.

HUVECs were seeded in 6-well plates and grown to confluence. A uniform scratch was created across the cell monolayer using a sterile 200 μL pipette tip. After washing with PBS to remove detached cells, fresh serum-free medium containing VEGF165 (2 ng/mL) and Ang-2 (2 ng/mL) was added, followed by treatment with RING1 or RING2 peptides (120 μM , diluted in culture medium with 1% DMSO). Images were captured at 0 and 24 hours post-treatment using phase-contrast microscopy. Wound closure (%) was calculated by measuring the gap area using ImageJ.

Transwell chambers (8 μm pore size; Corning) were used to assess cell migration. HUVECs (1×10^5 cells/well) were suspended in serum-free medium with VEGF165 and Ang-2, and seeded into the upper chamber. The lower chamber contained complete medium supplemented with 10% FBS. Cells were treated with RING1 or RING2 (120 μM) and incubated at 37 $^{\circ}\text{C}$ for 24 hours. Non-migrated cells were removed, and migrated cells on the lower membrane were fixed, stained with crystal violet, and imaged. Migrating cells were quantified using ImageJ.

Matrigel (Corning, 356234) was pre-coated onto 96-well plates (50 μL /well) and allowed to solidify at room temperature for 30 minutes. HUVECs (1×10^4 cells/well) were seeded on the gel and incubated with RING1 or RING2 (120 μM) for 6 hours. Capillary-like structures were imaged using a fluorescence microscope after Calcein AM staining. The number of junctions was quantified using ImageJ with the Angiogenesis Analyzer plugin.

Western Blot.

To assess the effect of peptide treatments on downstream signaling pathways, HUVECs were seeded into 6-well plates and cultured until approximately 50% confluence. Cells were then treated with RING1 or RING2 peptides (120 μM , medium: DMSO = 99:1 v/v) for 24 hours in the presence of VEGF165 (2 ng/mL) and Ang-2 (2 ng/mL) to simulate a pro-angiogenic microenvironment. After incubation, cells were washed with cold PBS and lysed with RIPA buffer containing protease and phosphatase inhibitors.

The protein content was usually determined using a BCA kit (Solarbio, PC0020). Each protein sample (50 μg) was subjected to 10% sodium dodecyl sulfate-polyacrylamide (SDS-PAGE) gel electrophoresis, and then transferred to a polyvinylidene fluoride (PVDF) membrane. The membrane was blocked with a blocking buffer (Xinsaimi Biotechnology, P30500). The membrane was incubated overnight at 4 $^{\circ}\text{C}$ on a shaker with primary antibodies against phosphorylated extracellular signal-regulated kinase (pERK), extracellular signal-regulated kinase (ERK) (Proteintech, 28733-1-AP/66192-1-Ig), phosphorylated protein kinase B (pAKT), protein kinase B (AKT) (Proteintech, 66444-1-Ig/10176-2-AP), and glyceraldehyde-3-phosphate dehydrogenase (GAPDH) (Solarbio, K200057M). The membrane was washed 3 times with Tris-buffered saline with Tween 20 (TBST), and then incubated with the corresponding secondary antibodies (Solarbio, SE134) (Solarbio, SE131) at room temperature for 1 hour. After washing as described above, the PVDF membrane was scanned on an Odyssey instrument.

Flow Cytometry Analysis of Immune Cells in Mouse Tumors.

The Renca tumor was cut into small pieces and digested in RPMI 1640 medium containing 1 mg/mL collagenase type IV at 37 $^{\circ}\text{C}$ for 1.5 hours. Then, the digested tumor tissue was filtered through a 70-micron cell strainer (Corning) and washed 3 times with pre-cooled PBS with 2% FBS. The samples were centrifuged at a low temperature, the cell suspension was counted, and according to the instructions of the reagent manufacturer, the cells were stained with antibodies such as anti-mouse V500-labeled CD45, BB700-labeled CD3, APC-labeled CD4, BB515-

labeled CD8, PE-labeled CD25, BV421-labeled FOXP3, and PE-labeled CD49b in a 4°C refrigerator for 60 minutes, and then analyzed using a flow cytometer. Finally, the stained cells were analyzed using a flow cytometer.

Enzyme-Linked Immunosorbent Assay (ELISA) Analysis of Tumor Tissues.

The tumor tissues after treatments were rinsed with pre-cooled phosphate buffered saline (PBS) to remove surface blood and impurities. Then, a certain weight of tumor tissue was chopped as finely as possible for sufficient homogenization. PBS containing a protease inhibitor (a 100-fold diluted solution of phenylmethylsulfonyl fluoride (PMSF)) (9 mL of PBS was added to 1 g of tissue) was added to the tissue, and it was thoroughly homogenized in a homogenizer. PBS containing PMSF (a 100-fold diluted solution) and a protease inhibitor (9 mL of PBS was added to 1 g of tissue) was added to the tissue, and it was thoroughly homogenized in a homogenizer. The homogenate was centrifuged at 5000g for 5 to 10 minutes at 4°C, and the supernatant was collected and analyzed using an enzyme-linked immunosorbent assay kit. The kits used included: (Solarbio, interferon- γ , SEKM-0031), (Solarbio, soluble intercellular adhesion molecule-1, SEKM-0132), (Solarbio, vascular cell adhesion molecule-1, SEKM-0037).

Plasma Stability Evaluation.

Frozen mouse/rat plasma was thawed and pre-incubated at 37 °C in a metal bath for at least 30 minutes. RING1-3 solutions were prepared (3mg/mL, water: acetonitrile =3:1, v/v). For the reaction setup, 100 μ L of each working solution was added to 900 μ L of pre-warmed mouse/rat plasma and vortexed for 5 seconds. Samples were incubated at 37 °C, and 100 μ L aliquots were collected at predetermined timepoints (0, 0.5, 1, 2, 4, 12, 24 h for rat plasma, 0, 15, 30, 60, 120, 240 min for mice plasma). Each aliquot was immediately transferred into a pre-chilled EP tube containing 200 μ L pure acetonitrile to terminate enzymatic activity and precipitate plasma proteins. Samples were centrifuged at 5500 g for 10 minutes at 4 °C, and the supernatants were transferred to high performance liquid chromatography (HPLC) vials and stored at 4 °C prior to analysis. HPLC analysis was conducted using a Zorbax SB-C18 Narrow Bore column equipped with a Phenomenex C18 guard column (4 mm \times 2.0 mm, 5 μ m). The mobile phase consisted of solvent A (0.1% formic acid in water) and solvent B (0.1% formic acid in acetonitrile), with a gradient elution: 5% B at 0 min to 90% B at 25 min. The injection volume was 70 μ L. Drug concentrations were quantified by peak area at the retention time corresponding to each compound. The percentage of compound remaining at each timepoint was calculated by subtracting the blank plasma signal and normalizing to the 0 min sample. The natural logarithm of the remaining percentage was plotted against time to perform linear regression, and the first-order degradation rate constant (K) was determined. The plasma half-life (T_{1/2}) was calculated using the equation: T_{1/2} = 0.693/K.

In vivo Tumor Model and Treatment.

For Renca subcutaneous tumor model, female BALB/c mice (6-8 weeks old, 18-22 g) were subcutaneously inoculated in the right flank with 5×10^6 Renca cells suspended in 50 μ L PBS with addition of 50 μ L matrix gel. Once the tumors reached 100 mm³ (about day 14 post-inoculation), mice were randomly divided into five groups (n = 5): PBS, RING1, RING2, RING3, and Axitinib + anti-PD-L1 antibody. RING1-3 were administered intravenously at a dose of 20 mg/kg (200 μ L, PBS) every other day for a total of five doses. Axitinib (5 mg/kg, orally) and anti-PD-L1 antibody (5 mg/kg, intravenously) were administered every 4 days for a total of 3 times. Tumor volumes and body weights were measured every two days using the formula $V = L \times W^2/2$, where L is the longest tumor diameter and W is the shortest. To establish the orthotopic RCC metastasis model, mice were anesthetized with using isoflurane gas and placed in a lateral position. After a 5-7 mm skin incision along the left flank, the peritoneal cavity was opened to expose the left kidney. A 29-G needle was inserted right beneath the renal capsule, and 15 μ L Matrigel containing 1×10^6 Renca cells was slowly injected. A visible bleb (about 2 mm diameter) under the capsule confirmed successful implantation. Bleeding was controlled by compression, and the surgical site was sutured with 4-0 absorbable sutures. Mice were randomly grouped (n = 5 per group) and treated with the same five regimens as in the subcutaneous model, beginning on 5 days post-implantation. Tumor metastatic burden was monitored by endpoint histology. Survival was monitored throughout the metastasis model study, and Kaplan–Meier survival curves were plotted to assess treatment efficacy.

Biosafety Assessment.

For safety evaluation, BALB/c mice (6-8 weeks old, 18-22 grams) was treated with PBS, RING1-3 and Axitinib + anti-PD-L1 antibody using the same treatment regimens as described above. After treatment, the mice were sacrificed, and the serum, and major organs were collected. The serum was subjected to a blood biochemical analysis by Vital River Laboratory Animal Technology Co. Ltd. The major organs were harvested for histological analysis performed by Wuhan Servicebio Technology Co., Ltd. Slices for H&E were used to observe potential pathological changes in major organs.

Statistical Analysis.

All data are expressed as the mean \pm standard deviation (SD). Statistical significance was one-way ANOVA followed by Student's t-test. ***p < 0.001, **p < 0.01, *p < 0.05.

Ethics approval statement

The welfare ethics of the laboratory animals were in accordance. The collection and use of animal samples was approved by the Committees for Ethical Review of the Fourth Affiliated Hospital of Harbin Medical University (No. 2022-DWSYLLCZ-96).

Acknowledgements

We thank Professor Lu Wang and Dr. Jiaqi Wang for their contributions to material characterization. This work was supported by the National Natural Science Foundation (No. 82402347), the Heilongjiang Provincial Natural Science Foundation (No. PL2024H188), the National Key Research and Development Program of China (No. 2022YFA1205704), the National Postdoctoral Program for Innovative Talents (Category B, No. GZB20230185), the China Postdoctoral Science Foundation General Program (No. 2023M740945) and the Heilongjiang Province Postdoctoral Science Foundation (No. LBH-Z23029, LBH-Z24230), New Era Heilongjiang Outstanding Master's and Doctoral Thesis Projects (LYXL2024-063).

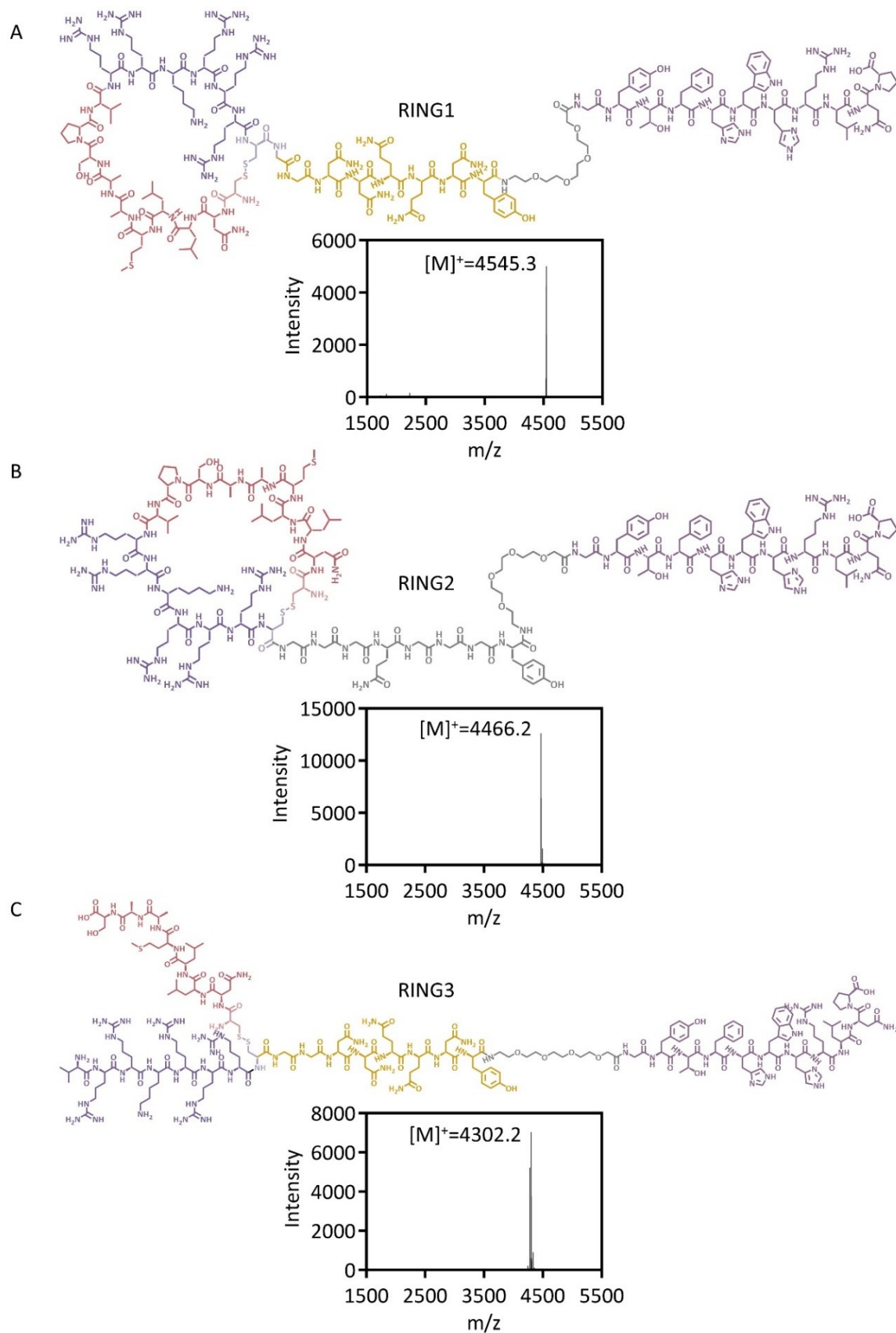


Figure S1. Molecular structures and mass spectra of RING1-3 peptide. The molecular structures are displayed: A) RING1 peptide, B) RING2 peptide, C) RING3 peptide and confirmed by matrix assisted laser desorption/ionization time-of-flight (MALDI-TOF) mass spectra.

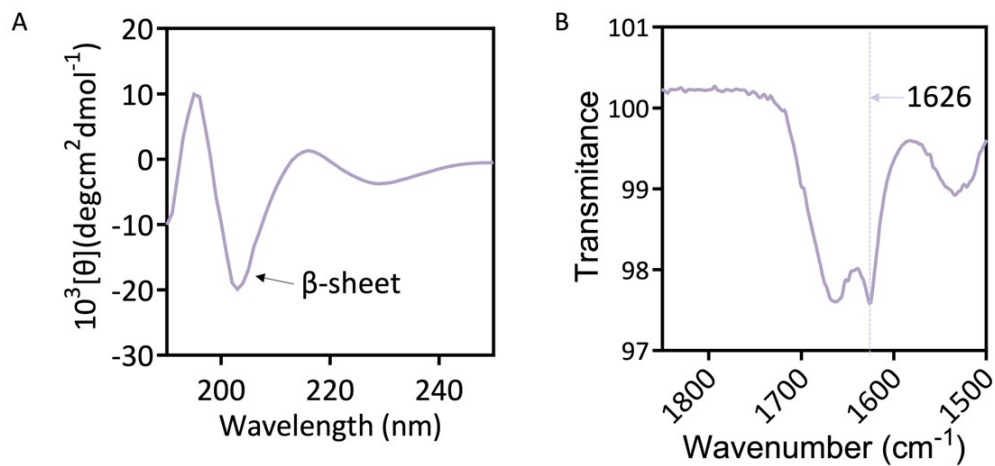


Figure S2. A) CD spectra of RING3 with incubation of Tie2 and VEGF, revealing protein-induced β -sheet structure. B) FTIR of RING3 with incubation of Tie2 and VEGF further confirming β -sheets structure in RING3 with assembly motif.

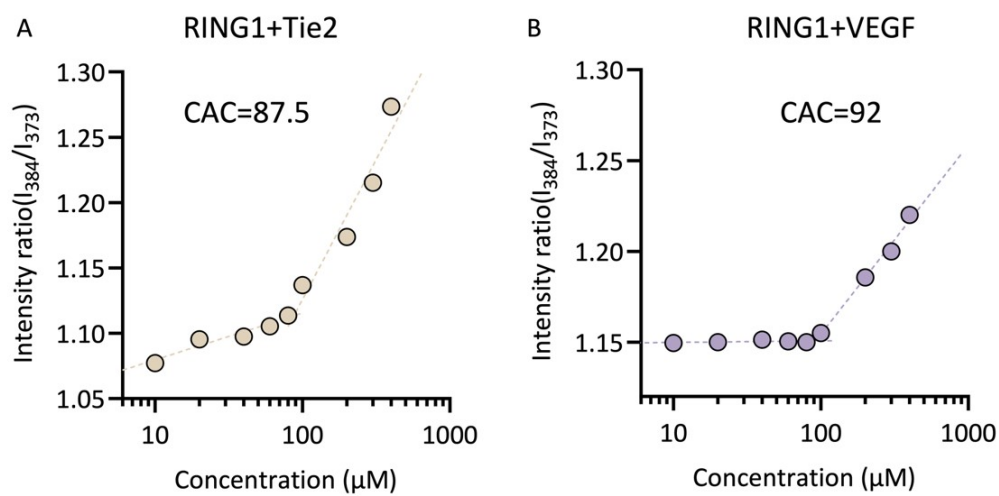


Figure S3. The CAC were carried out for the molecule RING1 under the induction of Tie2 (A) or VEGF (B) using pyrene fluorescence assays.

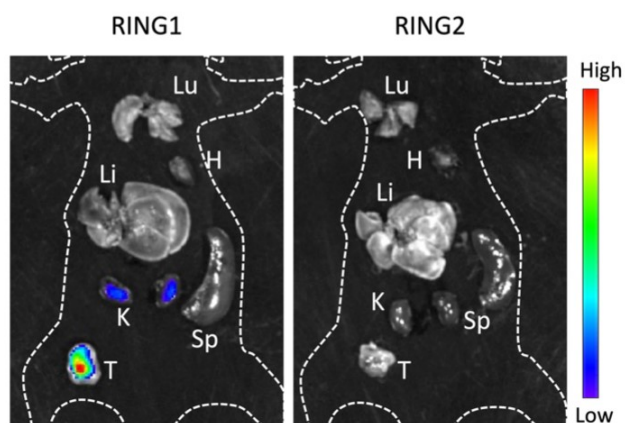


Figure S4. Ex vivo fluorescence imaging of tumors and major organs collected 12 hours after intravenous injection of Cy7-labeled RING1 or RING2 (400 μ M, 200 μ L). The fluorescence distribution highlights the preferential accumulation of RING1 in tumor tissue compared to other organs. H: heart, Li: liver, Sp: spleen, Lu: lung, K: kidney, Tu: tumor.

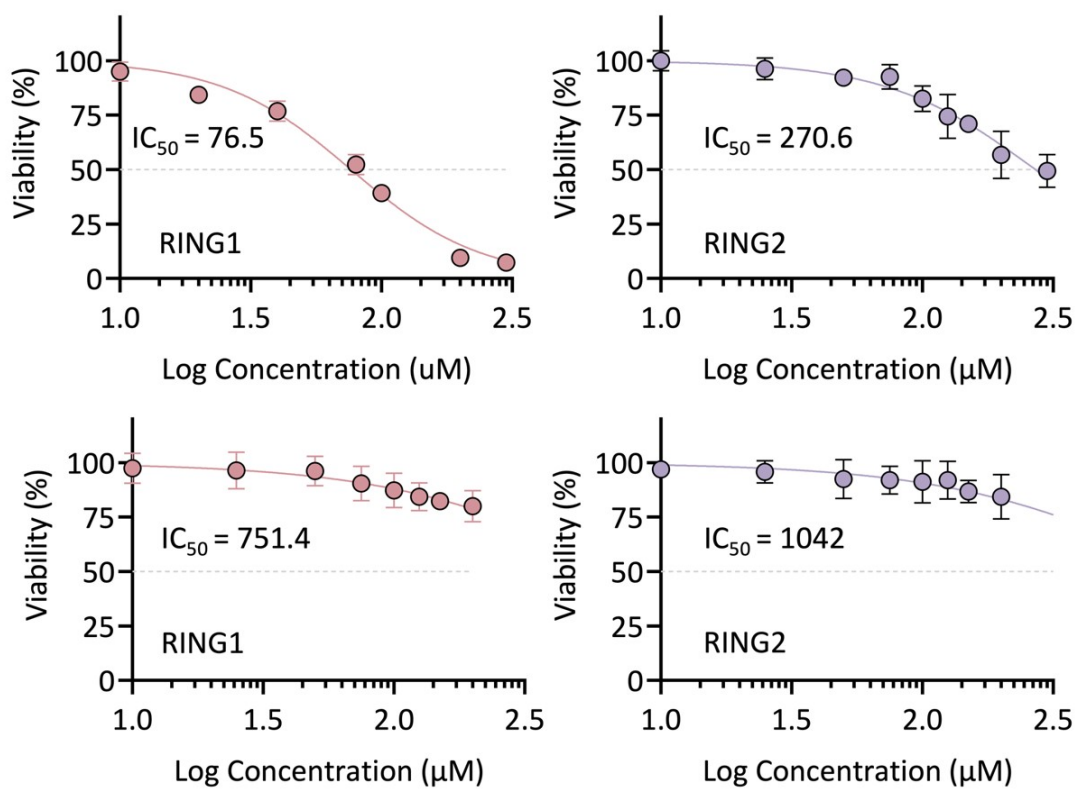


Figure S5. Cytotoxicity of RING1 and RING2. Cell viability was examined by an CCK8 assay in 786-O and 293T cells after the treatment with different concentration.

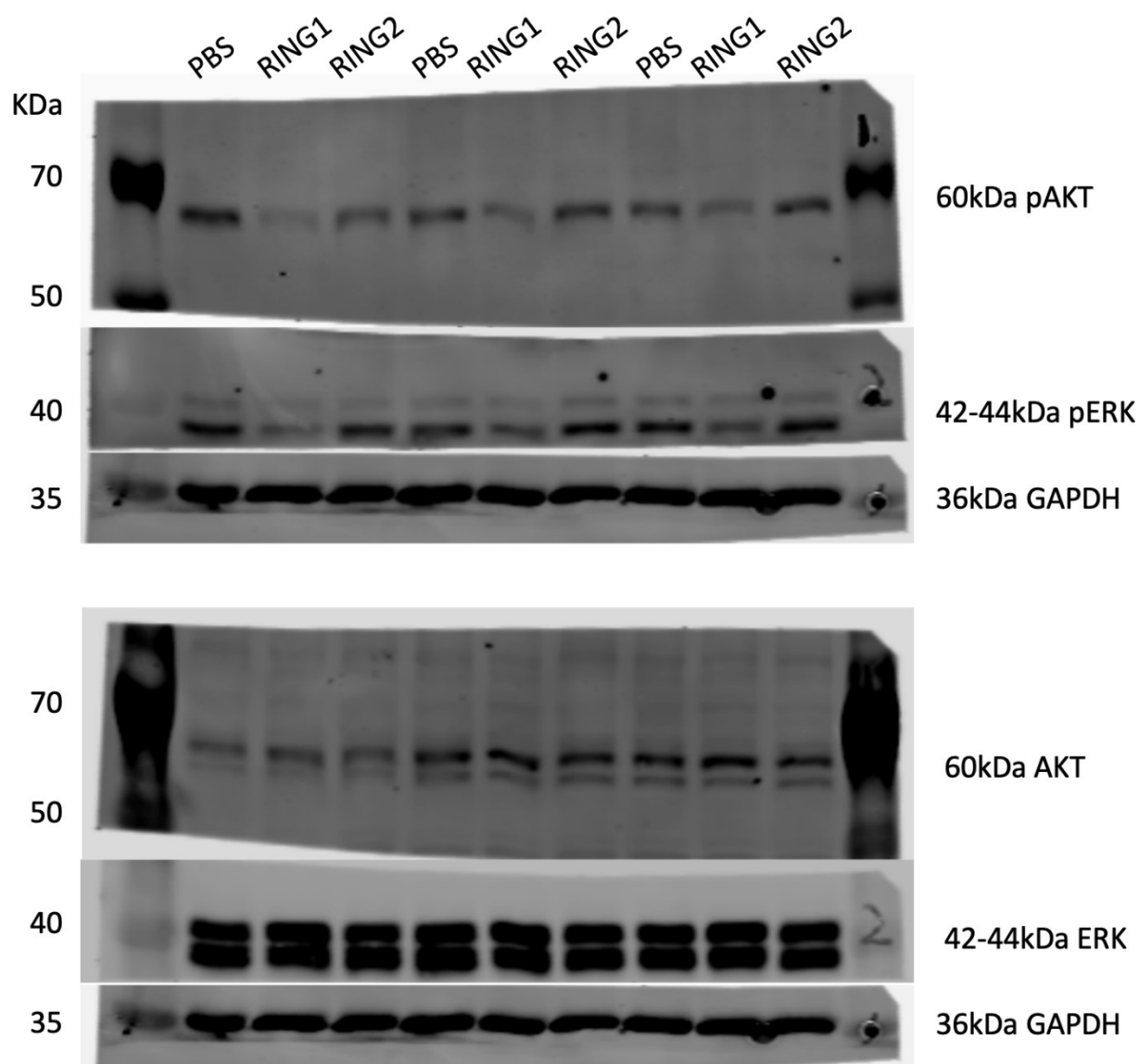


Figure S6. Western blot analysis of downstream signaling pathways following treatment with RING1/2 and PBS, including phosphorylated and total ERK and AKT.

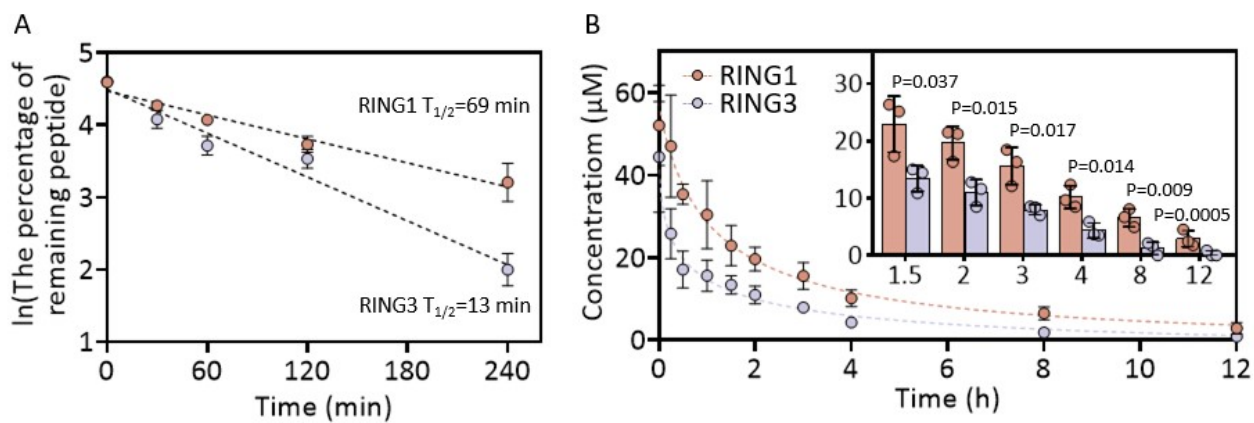


Figure S7. In vivo pharmacokinetics of RING1 and RING3 peptides. A) Stability of RING1 and RING3 peptides in mouse plasma, their plasma $T_{1/2}$ were 69 min and 13 min, respectively. B) Plasma concentration–time profiles of RING1 and RING3 following intravenous injection (200 μ M, 200 μ L, i.v), demonstrating the prolonged circulation and enhanced plasma stability of RING1.

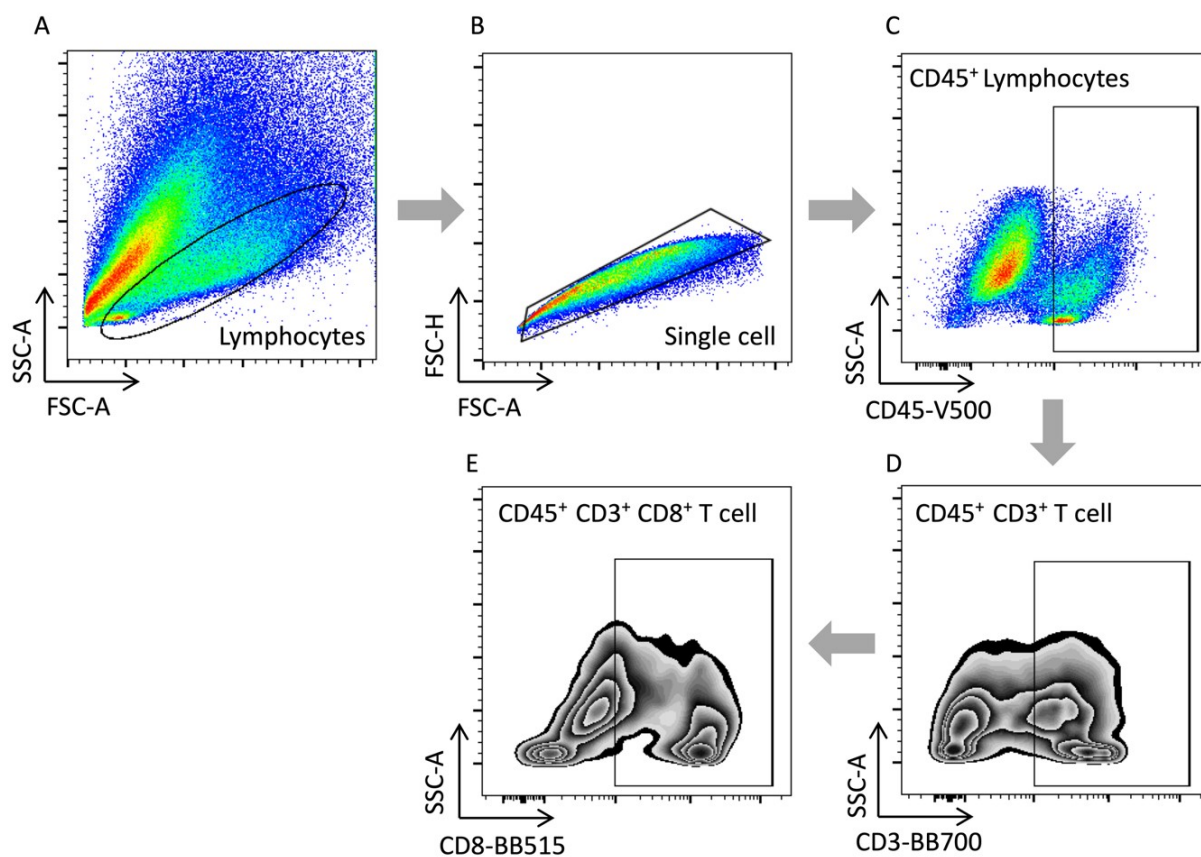


Figure S8. Gating strategy for T cell analysis in TME. Representative graph of whole sample with the gate showing lymphocytes (A), Representative graph of lymphocytes with the gate showing single cell (B), Gate showing lymphocytes gated as CD45⁺ cells (C), Gating showing CD45⁺CD3⁺ T cell (D), Gate showing CD45⁺CD3⁺CD8⁺ T cell (E).

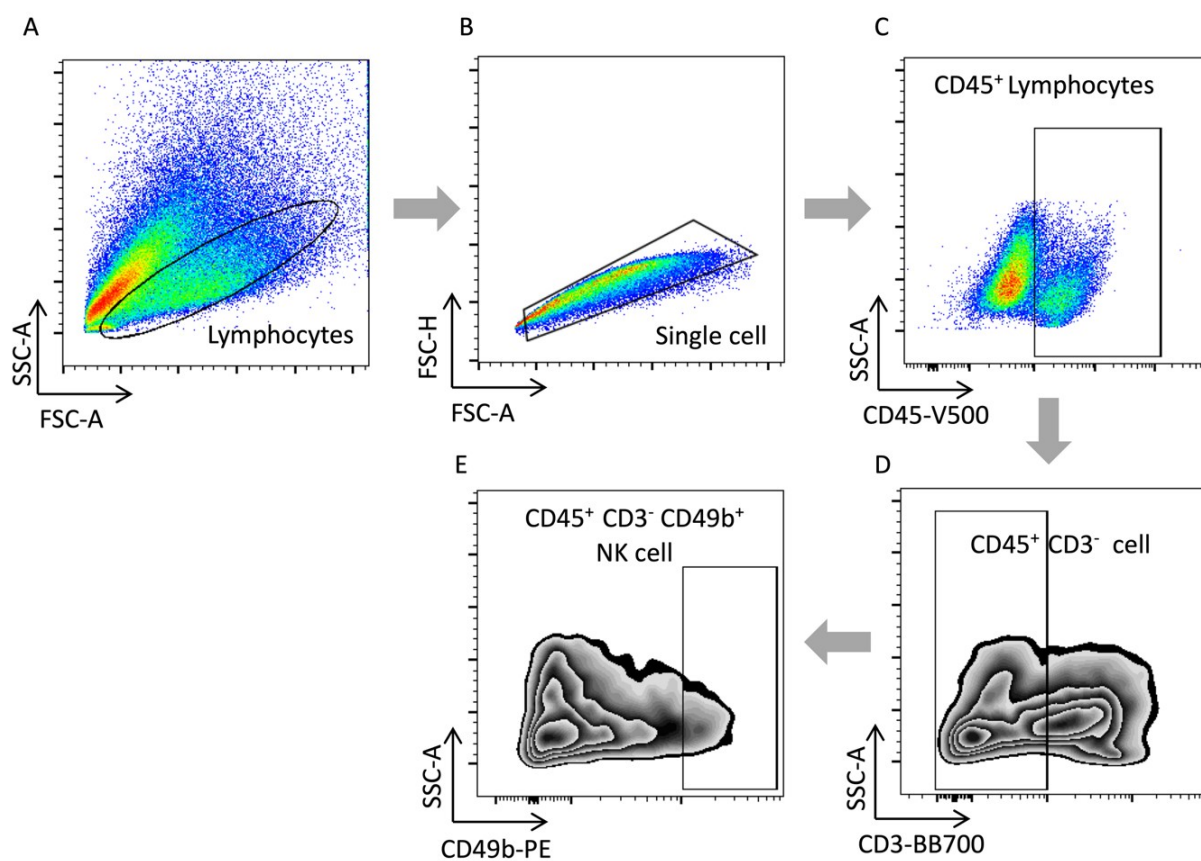


Figure S9. Gating strategy for NK cell analysis in TME. Representative graph of whole sample with the gate showing lymphocytes (A), Representative graph of lymphocytes with the gate showing single cell (B), Gate showing lymphocytes gated as CD45⁺ cells (C), Gating showing CD45⁺CD3⁻ cell (D), Gate showing CD45⁺CD3⁻CD49⁺ NK cell (E).

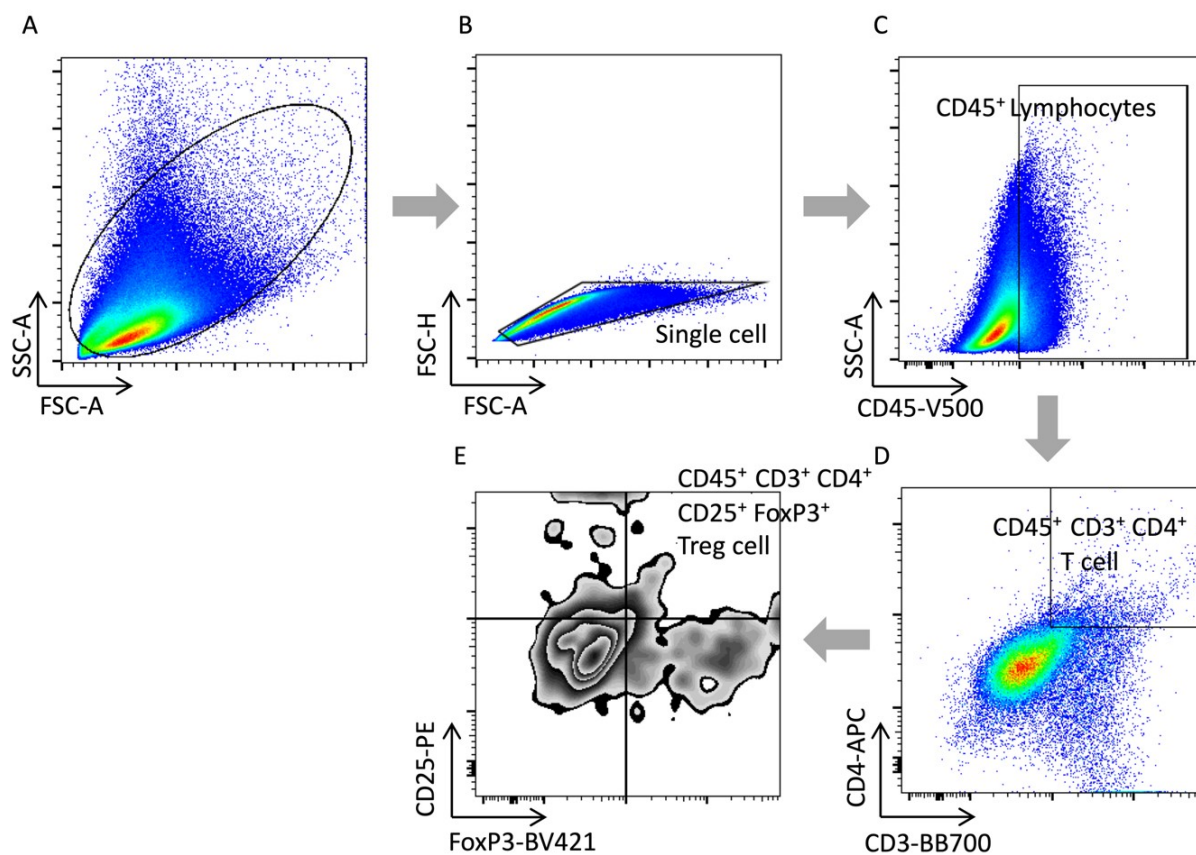


Figure S10. Gating strategy for Treg cell analysis in TME. Representative graph of whole sample with the gate showing main portion of cells (A), Representative graph of lymphocytes with the gate showing single cell (B), Gate showing lymphocytes gated as CD45⁺ cells (C), Gating showing CD45⁺CD3⁺CD4⁺ T cell (D), Gate showing CD45⁺CD4⁺CD3⁺CD25⁺FoxP3⁺ Treg cell (E).

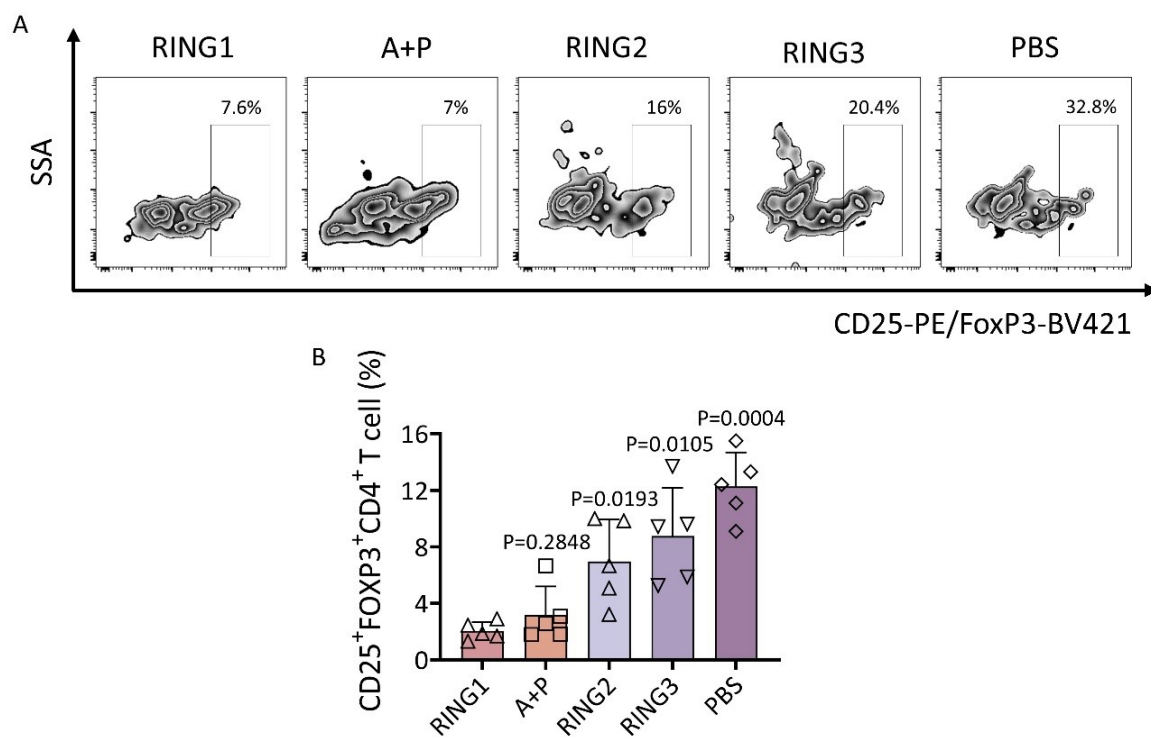


Figure S11. Representative flow cytometry analysis of CD4⁺CD25⁺FOXP3⁺ T cells (A) and corresponding quantification (B) in five different treatment groups (RING1, A+P, RING2, RING3, PBS) (n = 5).

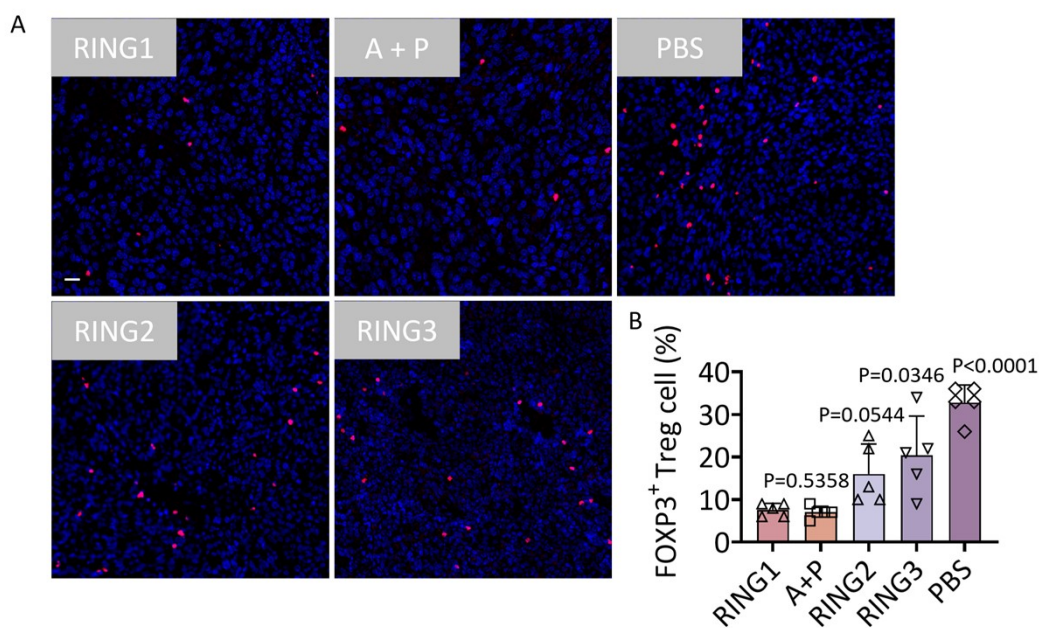


Figure S12. A) Representative immunofluorescence images of tumor sections from five treatment groups (RING1, A+P: Axitinib + PD-L1 antibody, RING2, RING3, and PBS). FOXP3⁺ regulatory T cells (red) and nuclei (DAPI, blue) were visualized to assess the counts of tumor-infiltrating Tregs (FOXP3⁺). Scale bar = 20 μ m. B) Quantification of the percentage of FOXP3⁺ T cells in tumor tissues (n = 5), showing that RING1 significantly reduced Treg infiltration compared to control and clinical combination groups.

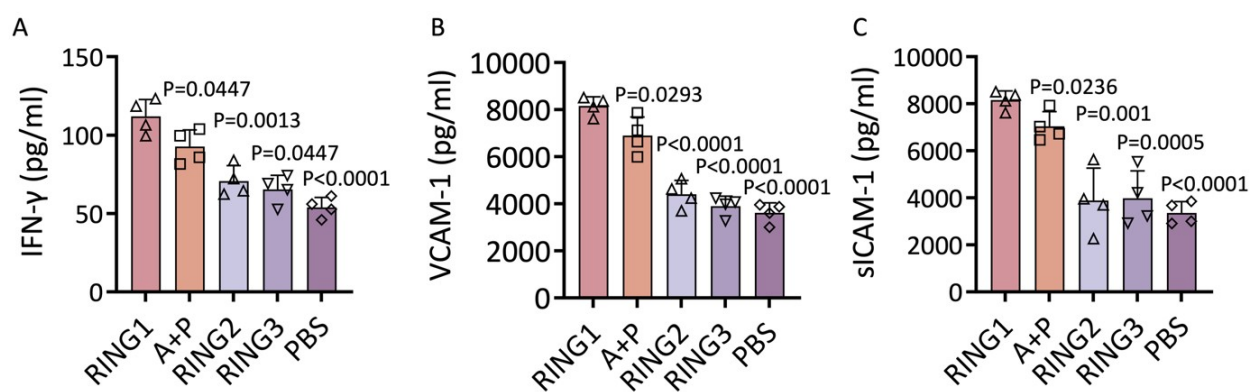


Fig. S13. The level of IFN- γ (A), VCAM-1 (B), sICAM-1 (C) in tumors of mice with the treatment of five groups: RING1, RING2, RING3 (each at 20 mg/kg, 200 μ L, i.v.), Axitinib + anti-PD-L1 antibody (A+P, 5 mg/kg per agent; axitinib orally, anti-PD-L1 via i.v.).

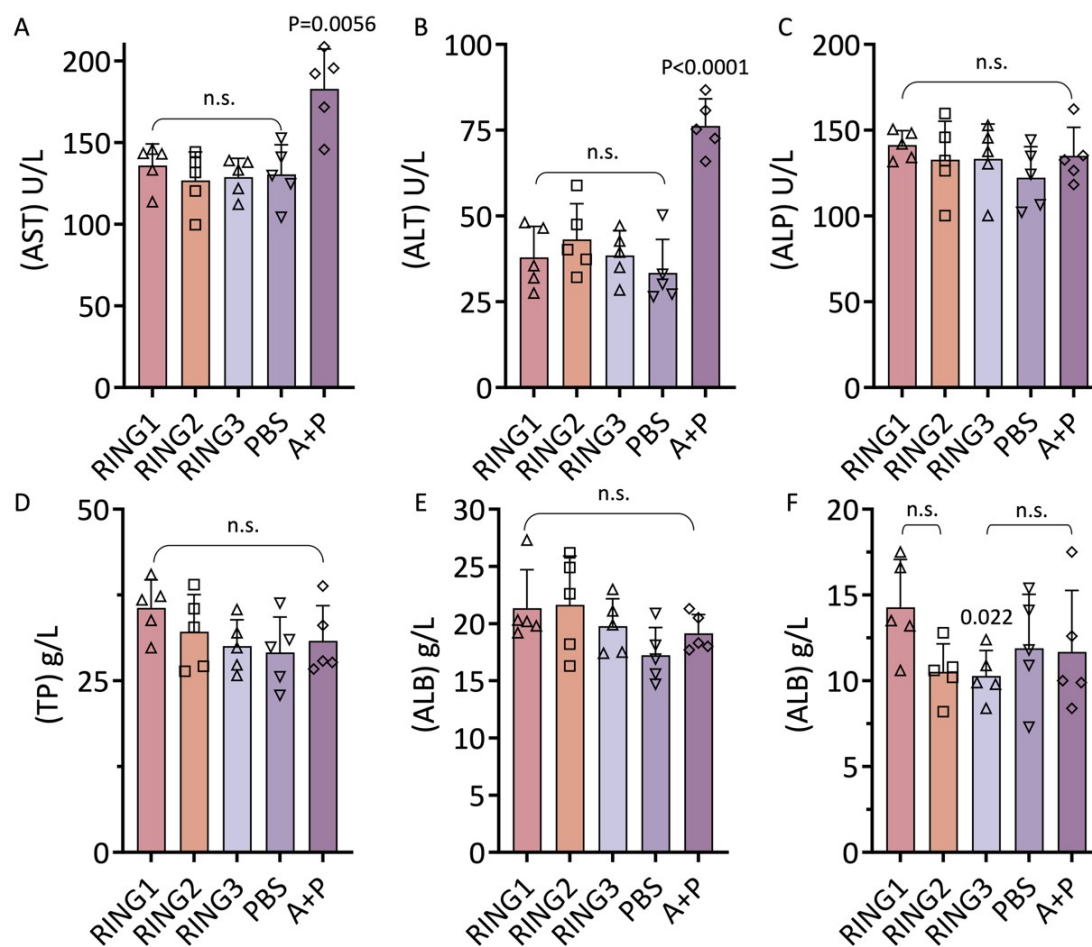


Figure S14. Serum markers of liver function in the five treatment groups (RING1, A+P, RING2, RING3, PBS): including aspartate aminotransferase (AST, A), alanine aminotransferase (ALT, B), and alkaline phosphatase (ALP, C), total protein (TP, D), albumin (ALB, E) and globulin (GLOB, F) levels (n = 5).

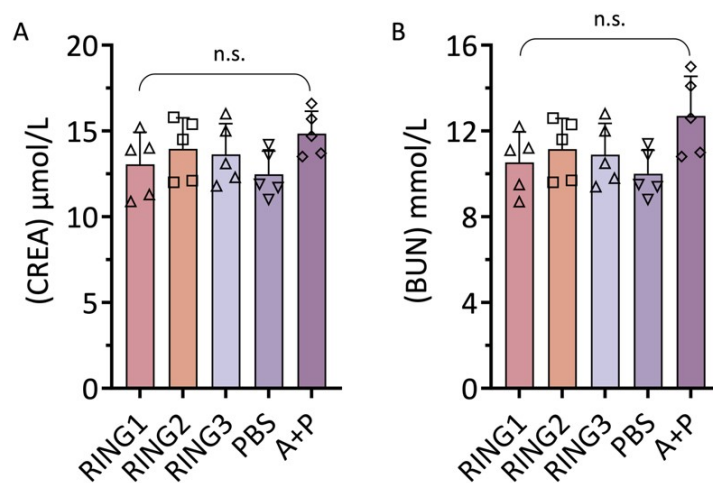


Figure S15. Serum markers of renal function in the five treatment groups (RING1, A+P, RING2, RING3, PBS): including creatinine (CREA, A) and the blood urea nitrogen (BUN, B) ($n = 5$).

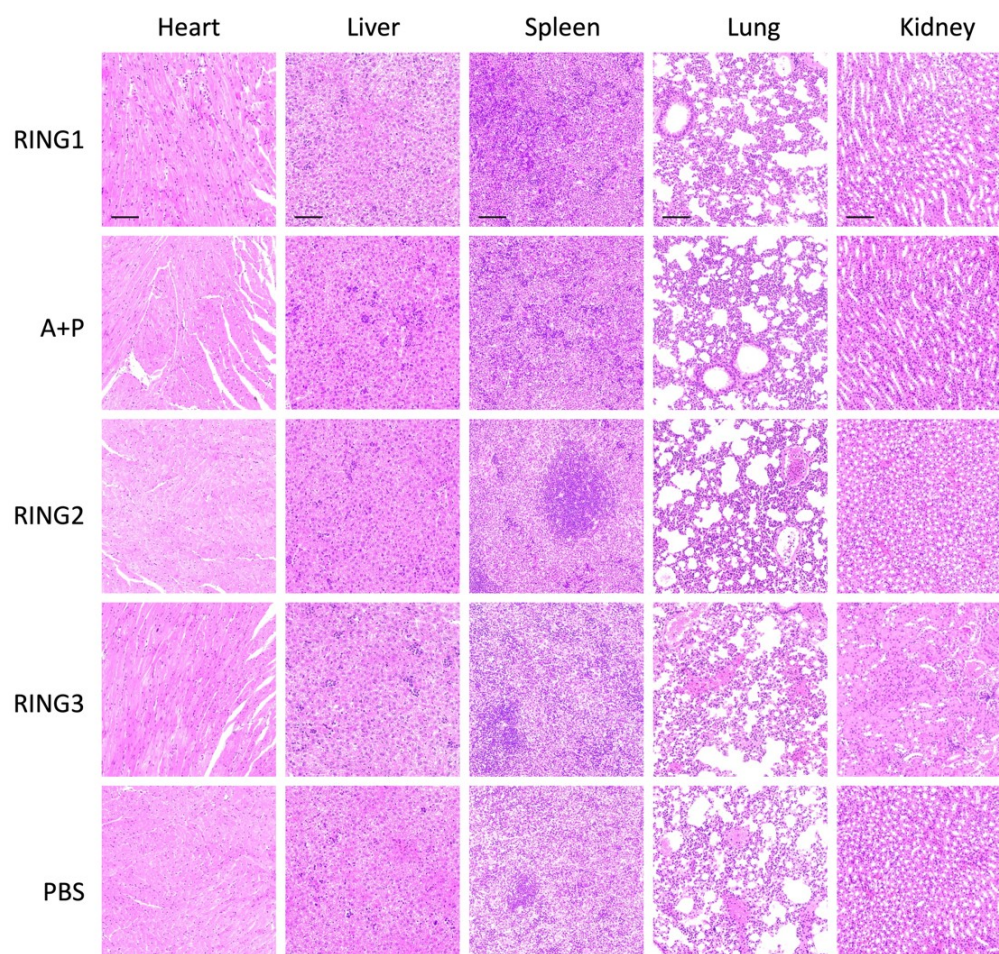


Figure S16. H&E staining of major organs including heart, liver, spleen, lung, and kidney collected from mice treated with different formulations (RING1, A+P, RING2, RING3, PBS).

Reference:

1. X. H. Zhang, B. L. Song, N. B. Yi, G. X. Zhang, W. F. Zheng, D. B. Cheng, Z. Y. Qiao and H. Wang, *Advanced Materials*, 2025, **37**.
2. B. L. Song, J. Q. Wang, G. X. Zhang, N. B. Yi, Y. J. Zhang, L. Zhou, Y. H. Guan, X. H. Zhang, W. F. Zheng, Z. Y. Qiao and H. Wang, *Angew Chem Int Edit*, 2024, **63**.
3. Y. Hao, D. Y. Hou, L. Zhou, Y. L. Fan, X. H. Wu, Y. X. Liu, Y. S. Xu, B. L. Song, L. Yi, Z. Y. Qiao, H. Wang and S. P. Xu, *Adv Mater*, 2025, **37**, e2413069.